COHERENT STRUCTURES IN ACCELERATING LOW REYNOLDS NUMBER JETS

Carlos B. da Silva and José C.F. Pereira
Instituto Superior Técnico,
Dep. Eng. Mecânica I (LASEF),
Av. Rovisco Pais, 1049-001 Lisboa, Portugal
csilva@navier.ist.utl.pt, jose@navier.ist.utl.pt

ABSTRACT

Direct Numerical Simulations (DNS) of spatially evolving, accelerating round jets are carried out in order to analyse the effects of acceleration on the coherent structures from the near field of round jets ($x/D < 10$). The acceleration is obtained by increasing in time the initial jet velocity, and thus the inlet mass flow rate, in a previously established *i.e.* steady jet. Here the focus is in low Reynolds number jets, where during the acceleration phase the Reynolds number increases from $Re_D = 500$ to $Re_D = 1000$. Only linear acceleration functions were considered and the acceleration parameter α ranges from 0.02 to 0.4. The primary structures found in the near field of the jet consist in axissymmetric (ring) vortices as in natural (*i.e.* non-excited) round jets with the same $R/\theta = 20$ ratio. However, for $\alpha \geq 0.02$ an helical arrangement ($m = 1$) is observed, and merging of the primary vortices takes place at about $x/D \approx 5 - 6$. For $\alpha \geq 0.1$ slip-trough events occur, in which the accelerating vortices overtake from inside slower/older vortices without ever merging to them. Detailed acceleration maps are used to track down the kinematics of the vortex motion in the near field of accelerating jets.

INTRODUCTION

The mixing and spreading rate of accelerating turbulent jets ($Re_D > 3 \times 10^3$) was studied experimentally by Kato *et al.* (1987) and Kouros *et al.* (1993), respectively. They observed that the mixing and entrainment of the jet are significantly modified by the acceleration when compared to the steady jet. In particular, the mixing was seen to depend not only on the jet velocity, but also on its time derivative *i.e.* the acceleration. In agreement with the theoretical predictions of Breidenthal (1986), Kouros *et al.* (1993) observed that the accelerated jet exhibits a much smaller spreading rate than the steady jet. It seems that the "entrainment appetite" of the near field structures is completely satisfied by the accelerating nozzle stream, thus reducing the spreading rate of accelerated jets. Zhang and Johari (1996) studied linear, quadratic and exponential accelerated jets with Reynolds numbers between $3 \times 10^3 < Re_D < 3 \times 10^4$. A reduced spreading rate was also observed in their measurements. As the flow accelerated a discernible "front" was established. Although this front travels much faster than the flow structures, they observed that for each acceleration rate the position of the front had the same functional form as the nozzle velocity. A model was developed to predict the time dependence of the front position. Finally, Johari and Paduano (1997) studied a gravity-driven jet where the jet velocity increases from zero to a maximum and then decreases continually. They observed that the acceleration/deceleration phase dilutes less/more than the steady jet, which seems to show that accelerating/decelerating jets spread less/more rapidly than steady jets.

Although the previous works allowed to shed some light into the phenomena of accelerating jets, the details concerning the large scale mechanisms have still to be described. In particular, those works gave no insight into the mechanisms of the near field coherent structures from accelerating jets, and how these could explain the reduced mixing and spreading rate of accelerated jets.

The present work uses direct numerical simulations (DNS) of low Reynolds number jets in order to analyse the dynamics of the near field coherent structures in accelerated jets. It is expected that a better understanding of these structures and their dynamics will lead to a better knowledge of accelerated turbulent jets. To the author's knowledge these are the first direct numerical simulations of accelerated jets.

NUMERICAL METHOD

The simulations were performed with an highly accurate Navier-Stokes solver in which the spatial derivatives are discretized using a 6^{th} order *Compact* scheme in the streamwise (x) direction and pseudo-spectral methods in the y and z directions. Temporal advancement is achieved with an explicit, 3 step, 3^{rd} order, low storage Runge-Kutta time stepping scheme and the incompressibility condition is insured by a fractional step method in which a Poisson equation is solved at each sub-step of the Runge-Kutta time stepping (for details see da Silva, 2001). All the computations were de-aliased using the 2/3 law.

In order to insure that the coherent structures leave the computational domain without being affected by the outflow boundary condition a non-reflective (Orlansky, 1976) outflow condition is used. This code was extensively validated in numerical simulations of round, plane and coaxial jets (da Silva and Métais 2002a,2002b, da Silva *et al.* 2003).

PHYSICAL AND COMPUTATIONAL PARAMETERS

Except for the Reynolds number and the details of the inlet velocity profile, all the simulations reported here are in all things equal to the simulation named "NLR" in da Silva and Métais (2002a). Therefore only a a brief description will be given here. All the simulations were carried out on the same mesh. The number of points is $201 \times 128 \times 128$ and the mesh size is uniform in all three directions. The computational do-

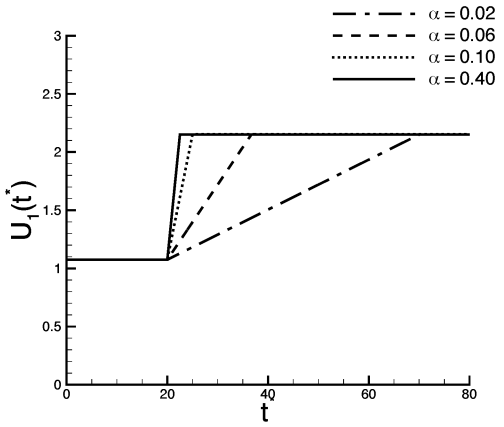

Figure 1: Temporal evolution of the maximum jet velocity for several acceleration parameters.

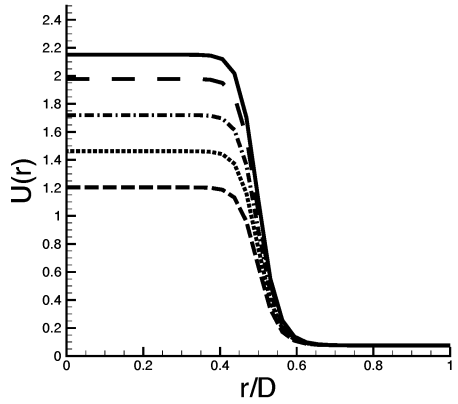

Figure 2: Evolution of the "mean" velocity profiles during the acceleration phase for $\alpha = 0.1$. The velocity profiles are separated by about $4t^*$.

main extends to $12.25D \times 7D \times 7D$ along the streamwise and the two transverse directions. The ratio of the jet radius to the initial shear layer momentum thickness is $R/\theta_0 = 20$ and the initial maximum jet velocity was $U_{01} = 1.075$.

Each time step t, a given velocity profile is prescribed at the inlet,

$$\vec{U}(\vec{x_0}, t) = \vec{U}_{med}(\vec{x_0}) + \vec{U}_{noise}(\vec{x_0}, t), \tag{1}$$

where $\vec{U}(\vec{x_0}, t)$ is the instantaneous inlet velocity vector. $\vec{U}_{med}(\vec{x_0}, t) = (U_{med}, 0, 0)$ is the mean streamwise velocity which is given by a hyperbolic-tangent profile (Michalke and Hermann, 1982)

$$U_{med}(\vec{x_0}, t) = \frac{U_1(t) + U_2}{2} - \frac{U_1(t) - U_2}{2} \tanh\left[\frac{1}{4}\frac{R}{\theta_0}\left(\frac{r}{R} - \frac{R}{r}\right)\right], \tag{2}$$

where $U_1(t)$ is the jet centreline velocity, U_2 is a small co-flow and θ_0 is the momentum thickness of the initial shear layer. The inlet noise profile $\vec{U}_{noise}(\vec{x_0}, t)$ is designed to set a small amplitude noise (1%) in the region of maximum shear layer gradient of the jet (see da Silva and Métais, 2002a).

Table 1: Non-dimensional time elapsed during the acceleration phase for each acceleration parameter.

α	Δt^*
0.02	50
0.06	17
0.1	5
0.4	2.5

The acceleration is obtained by imposing a temporal variation on U_1 in equation (2). The acceleration function has the following (linear) shape,

$$U_1(t) = U_{01}\,(1 + \alpha t)\,, \tag{3}$$

where α is the acceleration parameter and U_{01} is the initial maximum jet velocity, respectively.

Several DNS of accelerating jets were carried out with various acceleration rates α. Table 1 lists the values of α used and the non-dimensional time elapsed during the acceleration phase for each case. For each case, prior to the acceleration phase a steady jet with Reynolds number $Re_D = 500$ was established. Once a statistically steady jet is obtained, the acceleration described by equation (3) starts at a given time $t_0^* = t(U_{01}/D)$. Here we took $t_0^* = 20$. The acceleration is maintained until the Reynolds number reaches $Re_D = 1000$ (and $U_1(t) = 2U_{01}$). From that moment onwards, a steady jet is allowed to develop. Figures 1 and 2 illustrate the temporal evolution of the maximum velocity and the shape of the jet velocity profile. Notice that the ratio $R/\theta = 20$ is maintained throughout the acceleration phase.

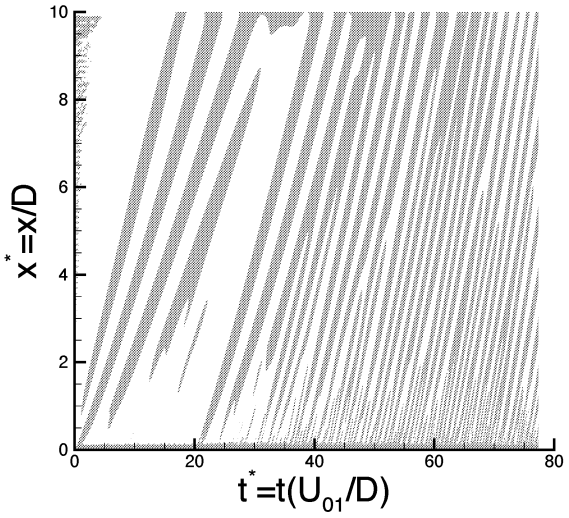

Figure 3: Acceleration map for the simulation with $\alpha = 0.02$, showing regions of $Q > 0$ (vortices) at several locations for each time instant.

RESULTS

In this study the focus is placed on the kinematics of the near field coherent structures of low Reynolds numbers accelerating jets. For the steady (non-accelerated) jet, the primary structures observed in our simulations consist in axis-symmetric (ring) vortices, as predicted by the linear stability theory when $R/\theta = 20$ (Michalke and Hermann, 1982) and as reported in numerous experimental and numerical works on round jets (*e.g.* da Silva and Métais, 2002a). Here the vortices are visualised using the so-called Q criterium, $Q = 1/2(\Omega_{ij}\Omega_{ij} - S_{ij}S_{ij})$, where Ω_{ij} and S_{ij} are the anti-symmetrical and symmetrical parts of the velocity gradient tensor, respectively. As in da Silva and Métais (2002a) we consider a vortex structure whenever $Q \geq 0.1(U_{01}/D)^2$.

For the steady jet at $Re_D = 500$, prior to the acceleration, the primary ring structures emerge with a characteristic frequency equal to $St_D = fU_{01}/D = 0.25$. This frequency corresponds to the jet *preferred mode*, and is a bit smaller than the value of $St_D = fU_{01}/D = 0.3$ obtained by da Silva and Métais (2002a) for $Re_D = 1500$. This can be explained by the effect of viscosity on the instability characteristics of the jet, still important for very small Reynolds numbers *i.e.* for $Re_D \leq 500$ (Morris, 1976).

Acceleration maps

In order to describe the complete vortex trajectories during a given simulation we define an acceleration map by writing Q along the shear layer zone of the jet ($0 < x/D < 10$ and $y/D \approx 1$), for each time step of the simulation. The location of the vortices is defined by a regions of $Q > 0$. A typical acceleration map, corresponding to the simulation with $\alpha = 0.02$, is shown in figure 3.

Two regions appear to be clearly divided. For $t^* = t(U_{01}/D) < 20$, the trajectory of the coherent structures has the same slope, which means that all the vortices are convected with the same (constant) speed. For $t^* = t(U_{01}/D) \geq 20$ the structures travel with an higher speed than before and are much closer to their neighbours. During the acceleration phase the trajectory of the vortices no longer has a constant slope but exhibits some curvature. This indicates that the velocity of each individual structure is also changing during the acceleration phase. When this curvature is "big enough" the trajectories of the vortices may intersect giving place to merging events where two or more vortices collide and form a new bigger structure. Merging between two or more vortices may occur. As an example, the figure 4 (top) shows a detail in the acceleration map for $\alpha = 0.02$ showing merging events between two vortices at $(t^*, x^*) \approx (39, 5)$ and $(t^*, x^*) \approx (44, 6)$. Three vortex merging were observed for $\alpha = 0.1$ as illustrated in the corresponding acceleration map at $(t^*, x^*) \approx (19, 1)$, $(t^*, x^*) \approx (21, 2)$ and $(t^*, x^*) \approx (24, 4)$.

Velocity time signal

Another feature observed in accelerating jets is the influence of the acceleration rate α to the response in the temporal evolution of the streamwise velocity component at the centreline. This is illustrated in figure 5. Notice that in both simulations the acceleration started at $t^* = 20$. It ended at $t^* = 70$ for $\alpha = 0.02$ and $t^* = 25$ for $\alpha = 0.1$. As expected there is a small time lag between the occurrence of the acceleration at the inlet and the response of the streamwise velocity

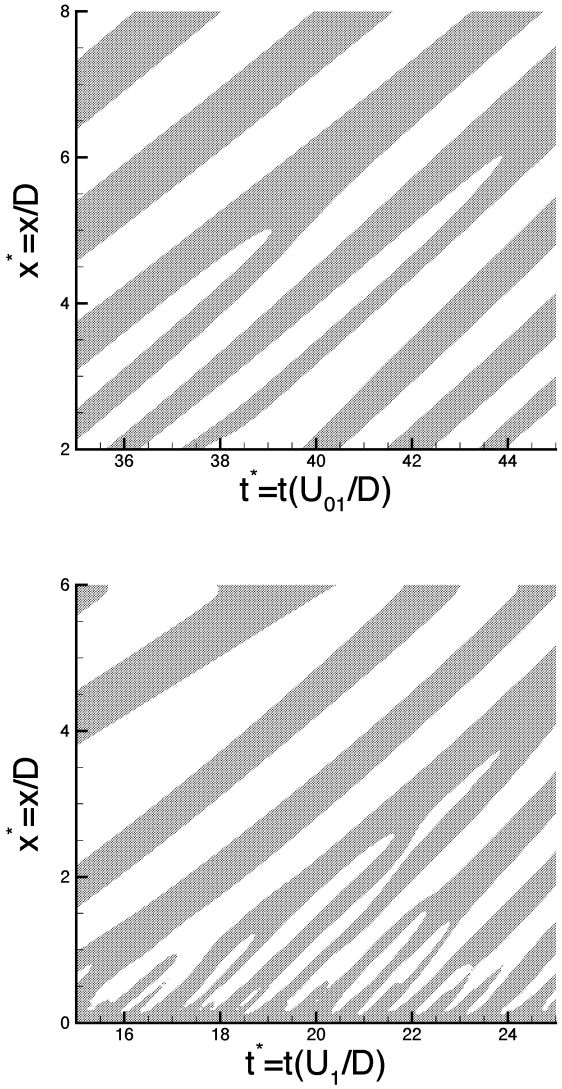

Figure 4: Detail of the acceleration maps for the simulations with $\alpha = 0.02$ (top), and $\alpha = 0.10$ (bottom), showing the merging between two and three vortices, respectively. (Note: for $\alpha = 0.10$ the acceleration started at $t^* = 10$.)

signal at $x/D = 3$ and $x/D = 6$. However, the acceleration causes the excitation of a given frequency in the velocity signal. It was observed that this frequency decreases with an increase in the acceleration rate, although the its amplitude tends to increase with α, at least for the small number of acceleration rates simulated in this work. The exact cause for this "additional" jet excitation caused by the acceleration is still under investigation. At the time of writing this paper it is not yet clear what near field vortex dynamics might trigger this excitation.

Visualisations

As stated above, before the start of the acceleration phase a steady jet is allowed to develop at $Re_D = 500$. The coher-

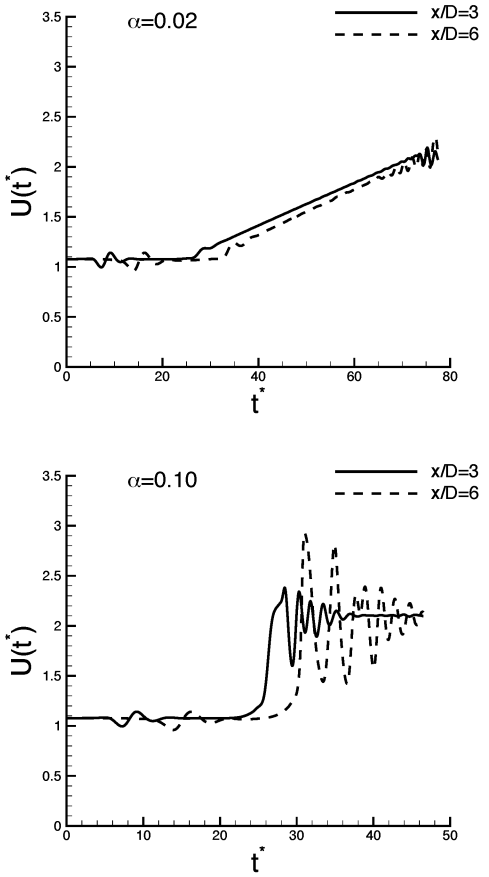

Figure 5: Temporal evolution of the streamwise velocity component at the centreline (at $x/D = 3$ and $x/D = 6$) in two simulations of accelerating jets with $\alpha = 0.02$ (top) and $\alpha = 0.1$ (bottom), respectively. For both cases the acceleration started at $t^* = 20$, however it ended at $t^* = 70$ for $\alpha = 0.02$ and $t^* = 25$ for $\alpha = 0.1$.

ent structures observed for this (steady) jet have the classical axissymmetric (ring) shape which results from the primary Kelvin-Helmholtz instability originated at the initial jet shear layer. The coherent structures observed during the acceleration phase depend on the acceleration rate α. For $\alpha = 0.02$ an helical ($m = 1$) arrangement appears sudently during the acceleration and maintains until the acceleration is stopped. The figure 8 (top) illustrates this case. Once the acceleration phase ends, and after some recovery time (which increases with the acceleration rate) the jet returns to the classical pattern of ring like structures separated by an almost constant distance between them. No merging is observed during this phase (at least for $x/D < 10$). The figure 8 (bottom) shows this phase for the simulation with $\alpha = 0.02$. A similar image characterises all the simulated jets after the recovery time.

For the higher acceleration rates $\alpha > 0.1$ a very interesting event takes place. It was observed that during the acceleration some newer/faster rings "slip-through" slower/older rings. This phenomena is illustrated in figure 8. During this process part of the vorticity of the newer/faster rings seems to be lost in the contact, which results in quite big slower/older

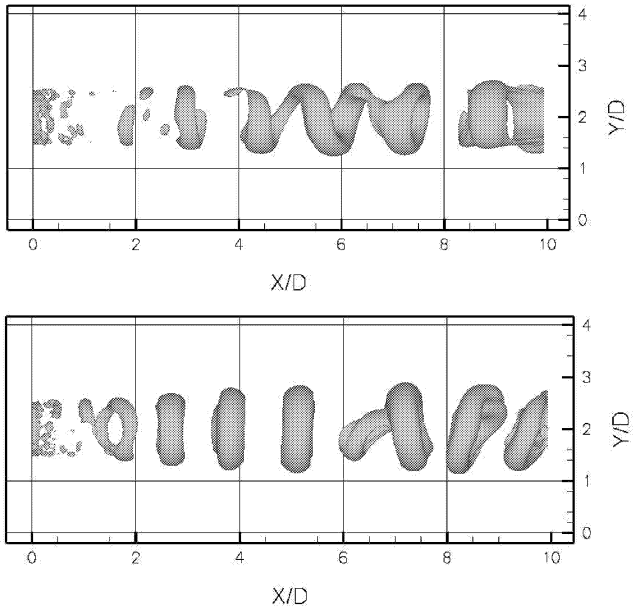

Figure 6: Isosurfaces of $Q = 0.1(U_{01}/D)^2$ for two instants from the simulation with $\alpha = 0.02$. During the acceleration (top); After the acceleration (bottom).

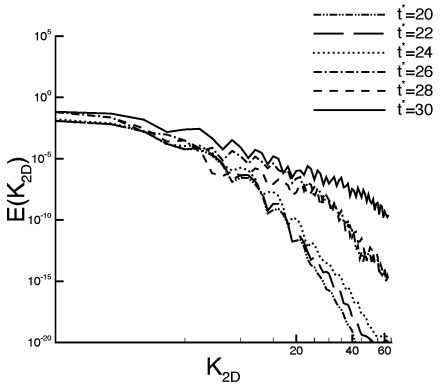

Figure 7: Two-dimensional (spatial) spectral at $x/D = 4$ at several times (during the acceleration phase) for the simulation with $\alpha = 0.1$.

rings. Careful analysis of these large scale events is underway and will eventually describe why do accelerating jets have reduced spreading rates compared to steady (non-accelerating) jets. As a future study we plan to carry out Large-Eddy Simulations (LES) to analyse the effects of acceleration in high Reynolds number jets.

Spatial 2D spectra

The figure 7 shows two-dimensional spatial spectra taken at $x/D = 4$ at several times during the acceleration phase for the simulation with $\alpha = 0.1$. The spectra show how does the small scale turbulence evolves during the acceleration phase. It is interesting to observe that the energy grows first at the large scales and only after do the small scales begin to show

more energy. This shows that it is some process related to the emergence of big structures (caused by the acceleration) that brings the growth of small scale turbulence. This is in contrast with the classical transition in jets, in which the energy begins to grow at the small scales level first.

CONCLUSIONS

Direct numerical simulations of accelerated low Reynolds number jets ($500 < Re_D < 1000$) were carried out in order to analyse the kinematics of the primary vortex rings resulting from the *preferred mode* instability, in the near field of round jets. The acceleration is imposed in a previously established steady jet.

The coherent structures existing in accelerated jets are axisymmetric (ring) vortices, as in the natural jet with the same $R/\theta = 20$. The main effect of the acceleration in the kinematics of these structures is to create velocity gradients between consecutive pairs of rings which causes events of merging and slip-trough. It was observed that in accelerated jets two or more vortices can merging into a bigger ring structure. Merging was observed for acceleration parameters greater than $\alpha \geq 0.02$. For $\alpha \geq 0.1$ slip-trough events take place, where a faster/younger ring overtakes a slower/older one from inside the ring.

REFERENCES

Kouros, H., Medina, R., and Johari, H., 1993, "Spreading rate of an unsteady turbulent jet", *AIAA Journal*, Vol. 31, pp.1524-1526.

Kato, S. M., Groenewegen, B. C., and Breidenthal., R. E., 1987, "Turbulent mixing in nonsteady jets", *AIAA Journal*, Vol. 25, pp.165-167.

Breidenthal, R., 1986, "The turbulent exponential jet", *Phys. Fluids*, Vol. 29, pp.2346-2347.

Zhang, Z., and Johari, H., 1996, "Effects of acceleration on turbulent jets", *Phys. Fluids*, Vol. 8, pp.2185-2195.

Johari, H., and Paduano, R., 1997, "Dilution and mixing in an unsteady jet", *Exp. Fluids*, Vol. 23, pp.272-280.

da Silva, C. B., 2001, "The role of coherent structures in the control and interscale interactions of round, plane and coaxial jets", *INPG*, PhD thesis.

Orlansk, H., 1976, "A simple boundary condition for unbounded hyperbolic flows", *J. Comp. Physics*, Vol. 21, pp.251-269.

da Silva, C. B., and Métais, O., 2002a, "Vortex control of bifurcating jets: a numerical study", *Phys. Fluids*, Vol. 14, pp.3798-3819.

da Silva, C. B., and Métais, O., 2002b, "On the influence of coherent structures upon interscale interactions in turbulent plane jets", *J. Fluid Mech.*, Vol. 473, pp.103-145.

da Silva, C. B., Balarac, G., and Métais, O., 2003, "Transition in high velocity ratio coaxial jets analysed by direct numerical simulations", *J. Turbulence.*, 4(024).

Michalke, A. and Hermann, G., 1982, "On the inviscid instability of a circular jet with external flow", *J. Fluid Mech.*, Vol. 114, pp.343-359.

Morris, P., 1976, "The spatial viscous instability of axissimetric jets", *J. Fluid Mech.*, Vol. 77, pp.511-529.

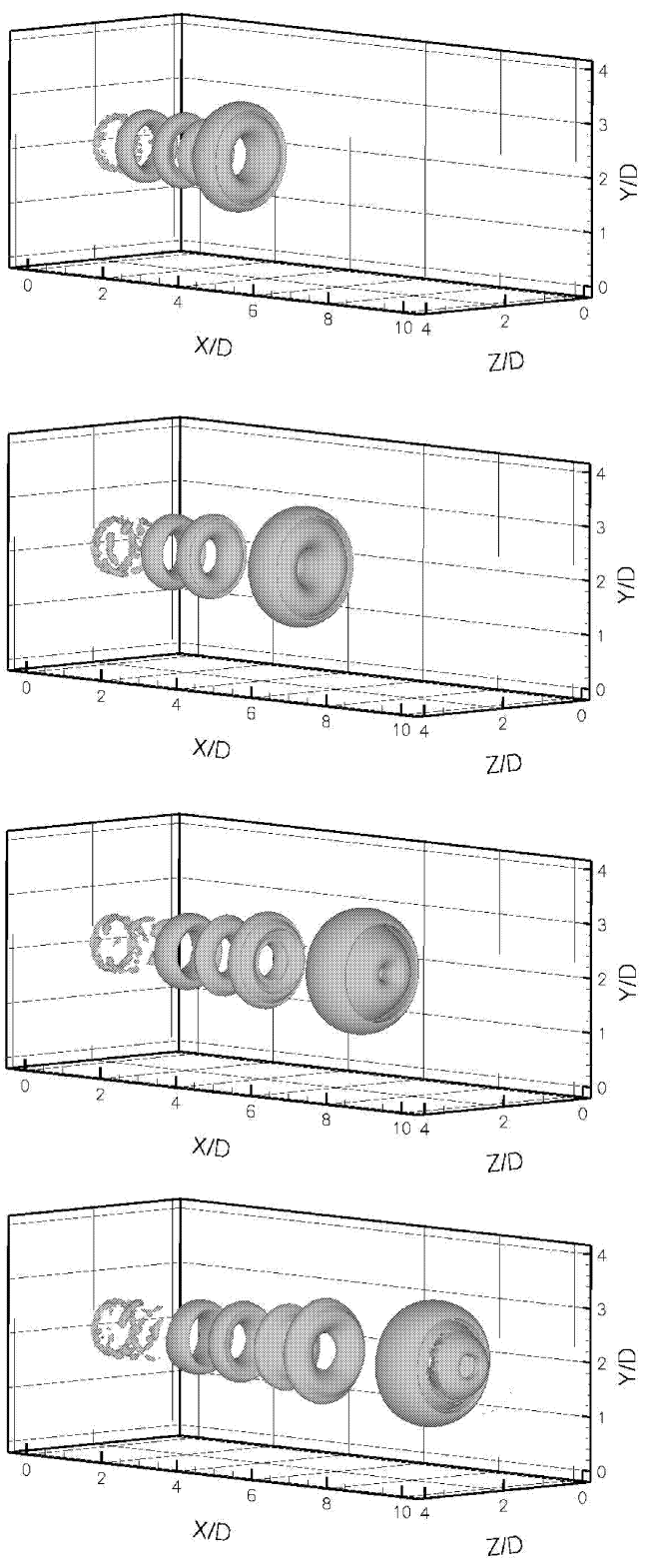

Figure 8: Isosurfaces of positive Q for four instants separated by about $2t^*$ for the simulation with $\alpha = 0.1$. The sequence is from top to bottom. The figures show a "slip-trough" event between the primary jet structures during the acceleration phase.